

A comparison of two Nextel 440 Fibre reinforced aluminium composites using acoustic emission

T. PACHECO, H. NAYEB-HASHEMI

Department of Mechanical, Industrial and Manufacturing Engineering, Northeastern University, Boston MA #02115, USA

H. E. M. SALLAM

Engineering Materials Department, Zagazig University, Zagazig, Egypt

The acoustic emission (AE) response and mechanical behaviour of two Nextel 440 fibre reinforced aluminium composites were compared. The total cumulative AE events were found to occur in two regions. The first region occurred at smaller strains and had a large exponential rise in events for the reinforced 6061 composite and few events for the high purity aluminium matrix composite. The difference was attributed to the alloy constituents of the 6061 aluminium matrix. The events were attributed to a dislocation release mechanism that occurred prior to yielding of the matrix. In the second region of events in the reinforced 6061 composite the event rate was constant and continued to failure. The second region of events in the high purity aluminium (HPAL) composite had a steady increase in the event rate until a constant rate was reached prior to failure. The events in the reinforced HPAL composite were attributed to the fracturing of fibres and the associated plastic deformation of the matrix that accompanies fibre failure. Thus failure in the materials occurs due to the propagation of fracturing fibres. The propagation was rapid in the reinforced 6061 aluminium composite. The reinforced HPAL composite had a slower propagation due to the high ductility of the HPAL.

1. Introduction

In recent years metal matrix composites (MMC's) have started to show some commercial acceptance. This is particularly true for composites with particulate reinforcement. Although MMC's have been under development for several decades, for continuous fibre reinforced metals to be accepted in the commercial market they still require significant development. The failure processes of the composites needs to be fully understood in order to improve the materials properties. Acoustic emission provides one means for understanding the failure mechanisms and thus may provide insight into the means for the improvement of the materials mechanical properties.

Acoustic emission (AE) is an emitted stress wave due to a release of energy in a system [1, 2]. The stress wave can be caused by any number of mechanisms that causes a redistribution of stresses in the system. Some possible sources of AE activity in MMC's are: fibre breaking, interface failure or debonding, interface cracking, friction or sliding, plastic deformation of matrix, and inclusion cracking.

There has been a considerable amount of research on AE in MMC's. Most of the research reports are on mono-filament (large diameter fibre) reinforced composites [3–5]. These reports relate the different types of damage occurring with the AE event peak ampli-

tude. The large amplitude signals can be correlated with the fibre breaking due to the high amplitude events that they generate. The event peak amplitude was found to increase with load, with a few high amplitude events occurring just prior to failure [5]. The rate of events was also found to increase with load to failure. Middle amplitude events were correlated with matrix deformation, without the various mechanisms being distinguished. Fewer studies are available that address AE in multi-filament (small diameter fibre tow) reinforced composites [6–8]. The smaller diameter of these fibres makes distinguishing events that are due to broken fibres difficult. Events with a large ratio of Ring Down Count (RDC) to Event Duration (ED) and mid to high amplitude have been attributed to fibre breaking [6]. AE has been associated with fracturing of the particle reinforcements in a particulate reinforced metal matrix composite [9]. In these reports little attention has been given to the identification of the various other sources of emission present in these composite materials.

There are a considerable number of reports of AE in metallic materials. The two primary sources of emission observed in metals are due to dislocation motion and the fracturing of inclusions. Dislocations have been shown to generate a large increase in AE activity just prior to the yielding. The activity then slowly

decreases after yielding [10–12]. The amount of AE has been shown to vary with different microstructures. Grain size has been shown to effect AE with a larger, sharper peak upon yielding in smaller grained materials [12, 13]. Precipitation strengthened alloys have been observed to generate significant amounts of activity upon yielding [10, 11]. From the data presented it appears that Gunnier Preston (GP(I)) zones may be a significant source of emission at the initiation of yielding. Cracking inclusions have been associated with copious amounts of AE in metals. The events generally associated with inclusions begin during yielding and continue to failure [14, 15]. A large peak occurring near yielding has been associated with the fracturing of inclusions [15, 16]. The observed peak may be due to more energy being released from larger inclusions, but it is likely that some activity is due to dislocation motion. The activity observed from inclusions has been shown to vary with a number of factors. The effect of lower yield stress was found to “completely eliminate burst acoustic emission activity” [17]. Changes in the orientation of the loading axis with the rolling direction has yielded different AE responses [15]. Twinning has also been observed to generate AE activity [14].

This paper is the second in a series on acoustic emission in metal matrix composites. The goal of this research is to gain some further insight into the failure processes and properties of the composites that are being manufactured at Northeastern University. Such understanding may help in determining possible routes for improving the mechanical properties of these composites. This paper compares the effects of two different matrices on the acoustic emission response and mechanical properties. One of the matrices is a high strength alloy with a low ductility and the other matrix has a low strength and is highly ductile. By comparing these effects further understanding may be developed on the damage that occurs in the composite.

2. Experimental procedure

2.1. Material

The composites used in this study were all reinforced with 3M's Nextel 440 fibres, the properties of which are given in Table I. The composites varied in matrix material, one matrix was a high purity aluminium (HPAL) and the other was the aluminium alloy 6061. The properties of the matrix materials are given in Table II for comparison. The high purity aluminium was 99.99% pure prior to casting. All of the com-

TABLE I Properties of Nextel 440 fibre 3M technical data sheet

Composition by W%		70%	Al ₂ O ₃
		28%	SiO ₂
		2%	B ₂ O ₃
Tensile strength	MPa (ksi)	2070	(300)
Modulus	GPa (ksi)	186	(27 000)
Elongation	%	1.1	
Diameter	µm	10–12	
CTE (25–500 °C)	10 ⁻⁶ /°C	4.38	
Shape		oval	

TABLE II Matrix properties [25]

		99.99% Al (annealed)	6061-T6 Al
UTS	MPa (ksi)	44.8 (6.5)	310.3 (45)
Yield strength	MPa (ksi)	10.3 (1.5)	275.8 (40)
Elongation	%	50	12

posites tested were manufactured at Northeastern University using a liquid metal pressure casting method. The nominal thickness of the 440/6061 composite and the 440 fibre reinforced high purity aluminium (440/HPAL) composite were 2.03 and 2.29 mm thick respectively. The fibre volume fraction of the composite plates are typically about 50%.

The 440 fibre reinforced 6061 Al (440/6061) composite was given heat treatments in order to obtain improved properties. The HPAL is not heat treatable and therefore no heat treatments were given to the composites with this matrix. The 440/6061 composite specimens were solutionized at 550 °C for 60 min, followed by a water quench. The composite was then aged for 1 h at 203 °C.

Prior to machining into specimens, the plates were examined by performing ultrasonic c-scans on the material. This ensured that the material was free from defects. The specimens were machined from plates by slicing the plates into strips using a diamond wheel. The specimens were then machined into a dog-bone shape that has been used previously [18]. The machining was performed on an Numerical Control (NC) machine. The 440/6061 composite was machined using a carbide end mill. The carbide endmill could not be used to machine the 440/HPAL composite. This was due to the rapid tool wear that resulted in damage to the specimen. For this reason the 440/HPAL composite was machined using a diamond tipped endmill. The diamond tipped endmill had an increased tool life and resulted in less damage to the specimens.

All specimens had aluminium end tabs applied using a hot pressing operation. A Hydrosol adhesive was used to bond the end tabs to the specimens. The end tabs provide a means to grip the composite without damage to the composite, thereby preventing specimen failure from occurring in the grips.

2.2. Mechanical testing

All tensile testing was performed using an Instron servo-hydraulic testing system with analog controller. The load was measured using a 100 KN load cell whilst the strain was measured with an Instron 2620-826 extensometer, with a 25.4 mm gauge length and a travel of 2.54 mm. All tests were performed using stroke control with an extension rate of 0.00254 mm s⁻¹. The testing was performed at this slow rate to prevent AE event pileup.

2.3. Acoustic emission testing

The AE was monitored during all tests using an AET 5500 testing system with 60 dB preamps. Acoustic

emission signals were measured using two AET AC175L transducers that were attached to the specimen using spring clamps. The use of two sensors enabled unwanted external events to be filtered out by event location. The system gain was set at 20 dB giving a total gain of 80 dB. The threshold was set at 0.12 V automatic this results in an amplitude lower cutoff of 23 dB. The automatic setting allows the threshold setting to rise with background noise. The 60 dB preamps resulted in an upper cutoff 77 dB. AE parameters, including load and strain data, were recorded on a computer for post processing.

3. Results and discussion.

3.1. Material

Metallographic examination was performed, using an optical microscope, in order to understand possible sources of acoustic emission in the materials. The composites were mechanically polished using standard metallographic techniques. The 440/6061 composite was found to have inclusions segregated around fibres, Fig. 1. These inclusions appear to form interconnected networks throughout the composite. The strength of the composite may be effected by the inclusions, through either short range stress concentrations due to the incompatibility with the matrix or broken inclusions that will cause stress concentrations on the fibres. McCullough *et al.* [19] found interconnected networks in cast 6061 aluminium and a Nextel 610 fibre reinforced composite. These networks lead to premature failure of the 6061 alloy “at a strain to failure of 0.7%”. Fig. 2 shows a typical microstructure of the 440/HPAL composite that was also examined. Few inclusions could be found in this material. The inclusions observed in the 440/HPAL composite appeared to be similar to the inclusions in the 440/6061 composite, although there were significantly fewer inclusions in the 440/HPAL composite. A preliminary (EDS) analysis revealed that the inclusions are a compound of iron. The inclusions are believed to be introduced during material processing.

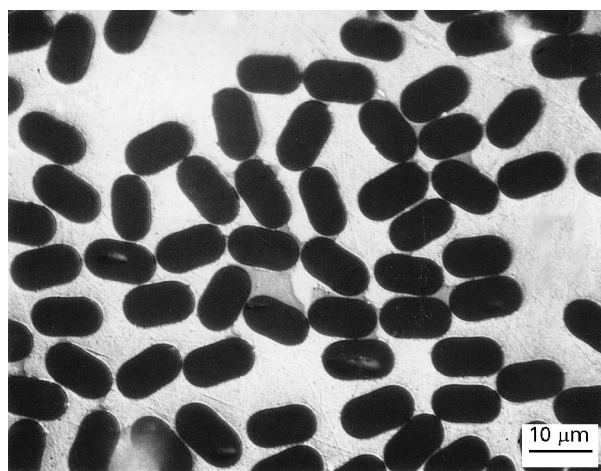


Figure 1 Photomicrograph of the 440/6061 composite showing fibres and inclusions, etched with sodium hydroxide solution.

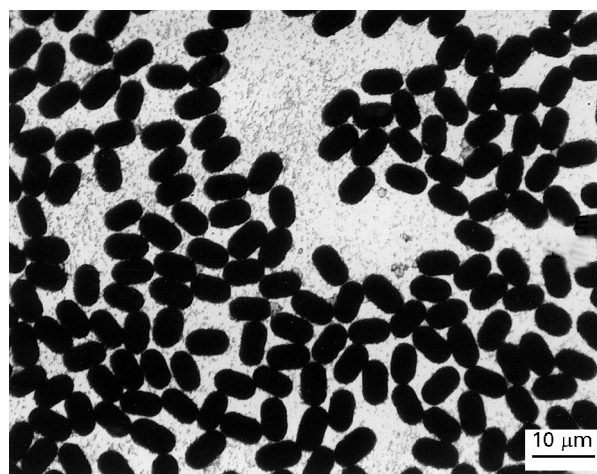


Figure 2 Photomicrograph of the 440/HPAL composite showing fibres and inclusions, etched with sodium hydroxide solution.

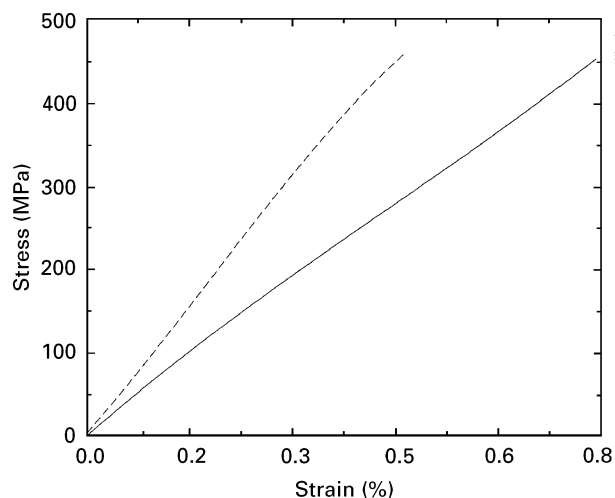


Figure 3 Stress versus strain for (---) 440/6061 and (—) 440/HPAL composites.

The fibre volume fractions were evaluated and found to be about 50% for both composites. During infiltration clustering of fibres occurs. This leads to regions depleted of fibres due to matrix channelling flow. The clustering also creates regions of high fibre volume fraction, typical volume fractions in these areas can be as high as 65%. The clustering of fibres and matrix channelling can have significant effects on composite behaviour.

3.2. Mechanical behaviour

Fig. 3 shows the stress–strain curves for the 440/6061 and the 440/HPAL composites. The 440/6061 composite has a bilinear stress versus strain curve. The transition in the curve occurs just prior to failure of the composite. Little plastic deformation of the matrix occurs before failure. The 440/HPAL composite also appears to have a bilinear stress versus strain curve. The transition occurs at a very small strain, or almost immediately in this material. The 440/HPAL composite undergoes a significant amount of plastic deformation compared to the 440/6061 composite. The tensile strength was found to be comparable for both

composites. The strength of the 440/HPAL composite appears to be slightly higher than that of the 440/6061 composite. The 440/HPAL composite also reached a much larger maximum strain prior to failure.

The strength of the composites are influenced by many factors. The statistical aspects of fibre properties can have significant effects on the composite behaviour and they govern the overall strength of the composite [20]. The composite strength is also dependent on the matrix strength, the matrix ductility, the bond strength and geometric effects [21–23]. These factors govern the damage propagation in the material. Bond strength affects the distances broken fibres require to transfer loads to the surrounding fibres. Based on the mechanical behaviour and the fracture surfaces of the composites the bond strength is considered to be strong in both materials. Improved wetting of the fibres is expected for the 6061 matrix due to the presence of Mg, which has also been shown to react with alumina fibres. Both of these factors increase the bond strength of the 440/6061 composite. The two composites compared have similar fibre volume fractions. The only other factors that influence the strength of the composites are the strength of the matrix, the matrix's ductility and defects present in the materials.

There are many sources of possible damage that may affect the composites strength. Inclusions have been found near or on the fibres in the 440/6061 composite. The presence of inclusions in the 440/6061 composite make it more susceptible to damage from the inclusions. Uneven or rough surfaces on fibres, due to reactions or bonding, may affect the strength of the fibres and hence the composite [24]. Stress concentrations on fibres from dislocation pileups are less likely to occur in the 440/HPAL composite due to the easier cross slip in this matrix. Therefore this source of damage should be more prominent in the 440/6061 composite. The 440/HPAL composite is more tolerant to damage. This can be evidenced from the larger strain at failure and the larger number of AE events, which can be considered to be an indicator of the damage occurring. This increased tolerance to damage is due to the softer matrix of the 440/HPAL composite which will more readily deform, slowing damage propagation and protecting the fibres.

The two composites were found to have similar strengths. The strength of the 6061 matrix is much greater. The higher strength of the matrix enables loads to be transferred quickly from broken fibres to surrounding fibres. This rapid transfer of load creates stress concentrations on the surrounding fibres, causing them to overload if the stresses are great enough. The 6061 matrix has a relatively low ductility which affects the behaviour of the composite. In composites with very low ductility matrices and strong bonding “the breakage of the weakest fibre and the composite occurred simultaneously” [21]. This is consistent with the observed behaviour of the 440/6061 composite in which few fibres were broken prior to the failure of the composite. The low strain to failure of the 440/6061 composite is consistent with a matrix dominated failure. Considering the low strength observed in the

440/6061 composite, a higher strength might be expected for the 440/HPAL composite due to the decreased strength and greater ductility of the matrix. These factors cause crack tip blunting and reduce stress concentrations on the fibres. In testing little improvement was found. This is due to the high density of fibres that allow load to be transferred rapidly from one fibre to another. The increased ductility and the weaker strength of the HPAL matrix slows crack propagation. The greater the ductility of the matrix the more fibres are needed to fail in order for fracture of the composite to occur [21]. Stress concentration are dissipated by the matrix slip in the weaker matrix [22]. This is consistent with the larger strain to failure of the 440/HPAL composite which approaches the strain to failure of the fibre. The loads in the fibres are also not high enough to lead to failure of the surrounding fibres. Once sufficient loads are reached the failure propagation can occur due to the high local fibre densities. There may be some increase in composite strength with increasing matrix ductility [21]. The higher fibre densities do not allow for the higher stress concentrations to be dissipated by the matrix. Significant stress concentrations can be transmitted to surrounding fibres when matrices have a high yield strength or in composites with a high volume fraction of fibres [20].

The elastic modulus of the 440/6061 composite was measured. From this the elastic modulus of the 440 fibres was calculated to be about 125 GPa by rule of mixtures, assuming a 50% fibre volume fraction and elastic matrix and fibres. This is about 33% lower than the published value. The reduction in stiffness comes from damage during processing. Reactions between fibres and matrix are one possible source of damage that could result in the decrease in fibre stiffness. The 440/HPAL composite has a very weak matrix and therefore the contribution of the matrix to the stiffness in this material is small. For this material the stiffness of the composite can be approximated by the contribution of the reinforcing fibres alone, using a 125 GPa fibre modulus. On the other hand the 440/6061 composite has a high strength matrix that can support significant loads. This leads to an increased composite stiffness due to the contribution of the matrix to stiffness which must also be considered in this material. The difference in stress of the two composites at the failure of the 440/6061 composite could be due to the contribution of stress in the matrix at that strain. This would be expected if the 440/HPAL composite is considered to be composed of elastic fibres in a plastic matrix and the 440/6061 composite having elastic matrix and fibres.

The tensile specimens were examined for broken fibres after testing. The matrix was partially dissolved in a HCl solution exposing the fibres in the gauge length. The fibres were then examined under an optical microscope for broken fibres away from the fracture surface. Some broken fibres were found in both the 440/6061 and 440/HPAL composites. In comparison more broken fibres were found in the 440/HPAL composite. The broken fibres appeared in small groups or bundles. This supports the prior conclusion

that more fibres are required to break in the 440/HPAL composite for failure to occur.

3.3. Acoustic emission

The total cumulative events versus strain are shown in Figs. 4 and 5 for the 440/6061 and 440/HPAL composites respectively. The AE events in the 440/6061 composite fall in two regions. The first region had an initial exponential increase in the number of AE events. The second region of events, following the exponential rise in events, the number of events increased linearly with strain until failure occurred. The 440/HPAL composite had a small number of initial events. After the initial events, the event rate slowly increased to a constant before failure of the material occurred.

The initial events in the 440/6061 composite occur incipient to yielding of the matrix and have been attributed to a dislocation activation mechanism [18]. Dislocations are believed to be initially pinned due to preferential precipitation around them. As the dislocations become active they create burst type emissions. This rise in events is also similar to that observed by Fang and Berkovits [14] in a 901 superalloy.

Comparison between the 440/6061 and 440/HPAL composites reveal a considerable difference in the

initial rates of AE events. The only significant difference between the two composites is that the 440/HPAL composite is not alloyed. This difference effects the behaviour of the material and hence the AE response. In the 440/HPAL composite the dislocations are not restrained by solute atoms or second phases, resulting in a weaker matrix and larger numbers of mobile dislocations. Due to the larger numbers of mobile dislocations the dislocations will need to move shorter distances and are therefore less likely to create detectable emission. For these reasons fewer initial events would be expected for the 440/HPAL composite. Some AE events may still be generated by dislocation motion when sufficient numbers move coherently within a small volume.

These differences in initial events between the two composites also reinforce conclusions previously made regarding the source of the initial AE activity in the 440/6061 composite. The events are due to dislocation sources and they become active due to changes in the ageing response of the 6061 matrix in the 440/6061 composite [18]. These changes in the ageing response are due to residual stresses generated upon cooling due to differences in the coefficient of thermal expansion and reactions of the alloy constituents with the fibres.

The second region of total cumulative events curve is nearly linear for both of the tested composites. Previous work on the 440/6061 composite resulted in the conclusion that the events in the second region are due to inclusion fracturing [18]. This conclusion was reached after comparison of AE events in a 6061 alloy with the 440/6061 composite. In addition it also was found that few fibres were broken in a specimen that had been loaded to about 90% of its ultimate tensile strength (UTS) and dissolved in HCl acid. Metallographic examination of the 440/HPAL composite revealed that there are few inclusions present in this material. For this reason, inclusions can not be considered to be a significant source of AE in this material. Other possible sources of emission in this material are fibre fracturing, interface failure, matrix plastic deformation (dislocation motion) and friction (fibre–fibre, fibre–matrix, matrix–matrix). The emission exhibited inclusion like behaviour and hence is believed to be due to fracturing fibres and some associated matrix plastic deformation. Fibres will fail due to stress concentrations on them. The fracturing fibres will also result in matrix plastic deformation in a small region surrounding the broken fibre. This localized plastic deformation in the matrix may generate additional AE activity.

The peak amplitude distributions were compared for the two composites tested, Figs. 6 and 7. The distributions are similar for both materials. There were only a few differences between the two materials. The sharp rise in events that occur in region 1 of the 440/6061 composite are predominantly lower amplitude events. The events in region 2 are of a similar amplitude but there is an increase in the number of higher amplitude events. These events can be seen in Fig. 8 which shows the cumulative events by peak amplitude. The similarity of event peak amplitude

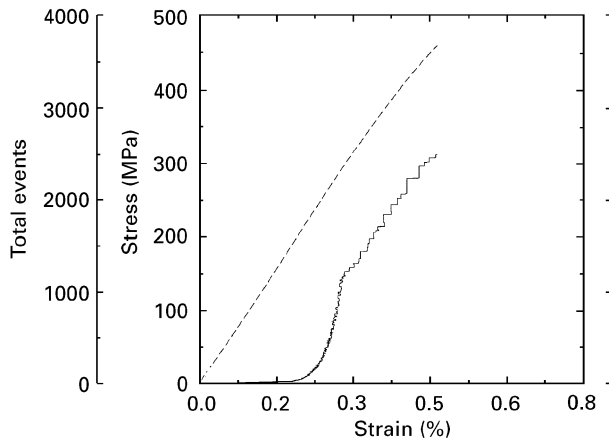


Figure 4 (---) Stress and (—) total cumulative events versus strain in the 440/6061 composite.

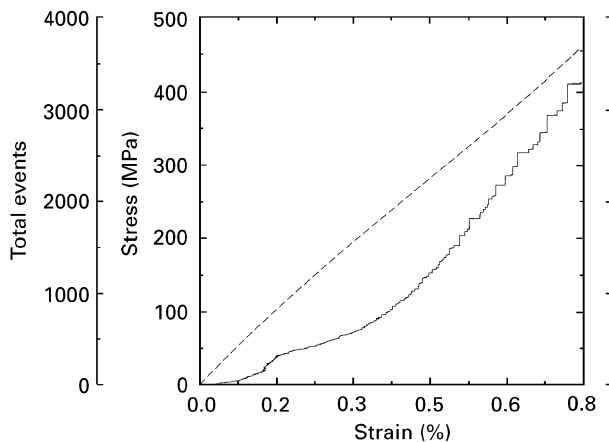


Figure 5 (---) Stress and (—) total cumulative events versus strain in the 440/HPAL composite.

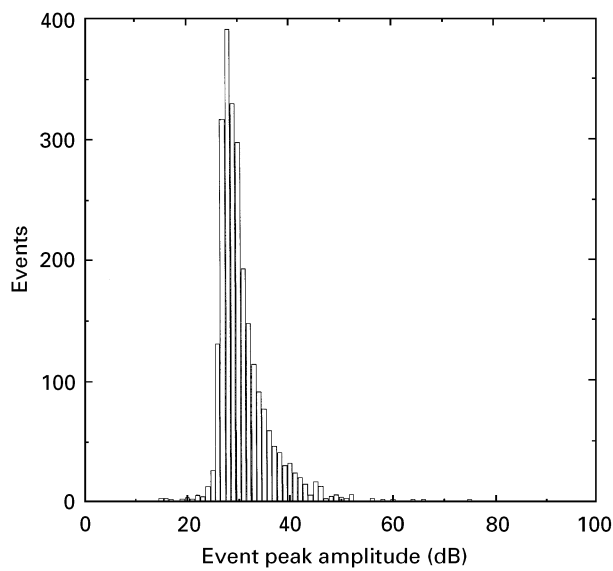


Figure 6 Distribution of events by event peak amplitude in the 440/6061 composite.

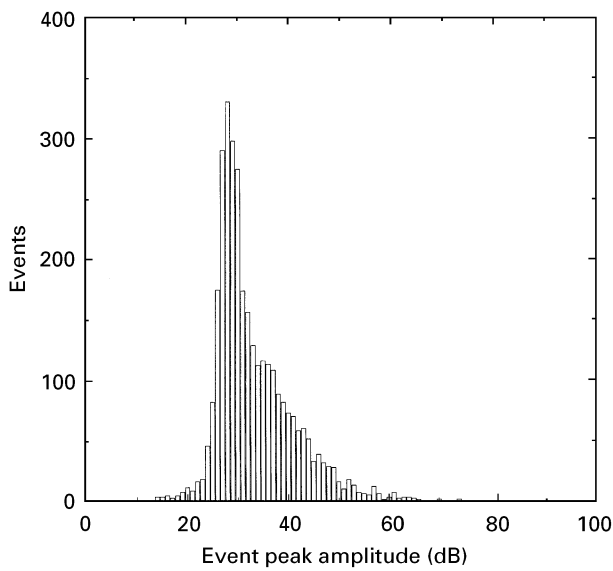


Figure 7 Distribution of events by event peak amplitude in the 440/HPAL composite.

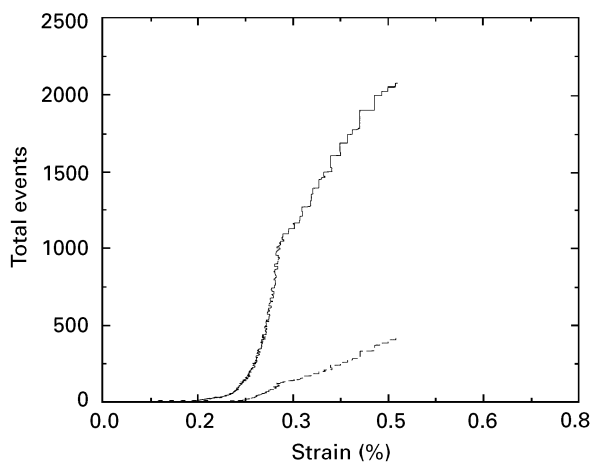


Figure 8 Cumulative AE events versus strain by peak amplitude in the 440/6061 composite. The key is: (—) PA < 35dB and (---) PA > 7, 35dB.

from one region to the next makes separation of event sources difficult. Other AE parameters, such as event duration, were compared with similar difficulties. The event distribution of the 440/HPAL composite is slightly broader with an increased number of higher amplitude events (dB > 35). Events due to fibre breaking have been attributed with a high event peak amplitude [6]. The increased numbers of higher amplitude events are consistent with events due to fibre breaking. Fibre breaking is also expected in the 440/HPAL due to the high matrix ductility and the large strain to failure of the composite that approaches the strain to failure of the fibre. The event peak amplitude observed is reasonable when considered that the size of the fibres breaking are small. For these reasons the higher amplitude events of the 440/HPAL composite are attributed to be due to fibre breaking. The lower amplitude events observed are attributed to be primarily due to matrix plastic deformation.

3.4. Fracture

The fracture surfaces of the composites were examined and compared. The fracture surface of the 440/6061 composite, Fig. 9, was found to be relatively flat with large planar terraces. There is limited matrix plastic deformation between the fibres and no significant fibre pullout. The fracture surface of the 440/HPAL composite, Fig. 10, has a greater amount of plastic deformation. The fracture surface is rougher and there is a larger number of terraces. There also appears to be a larger amount of fibre damage through fragmentation of fibres at the fracture surface. The fracture surface shows plastic necking of the matrices between the fibres. The necking is more considerable in the 440/HPAL composite due to the greater ductility of the composite's matrix. The 440/6061 composite has a flatter fracture surface that is composed of numbers of planar terraces. The flatness of the fracture surface is due to the rapid crack propagation through this material. The terraces are due to bundles of fibres or regions of high fibre volume fraction failing simultaneously. The rougher fracture surface of the 440/HPAL composite is due to the increased number

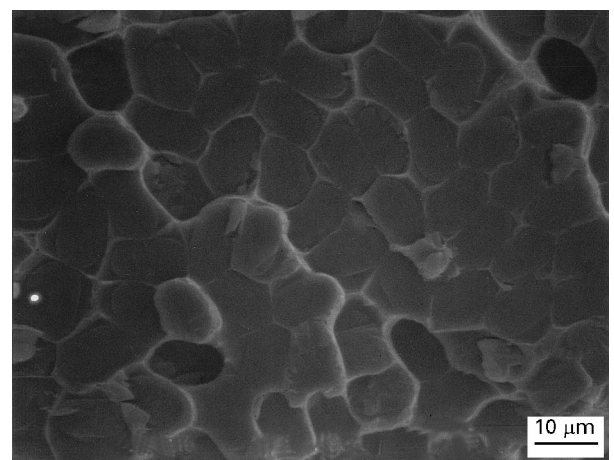


Figure 9 Fractograph of the 440/6061 composite.

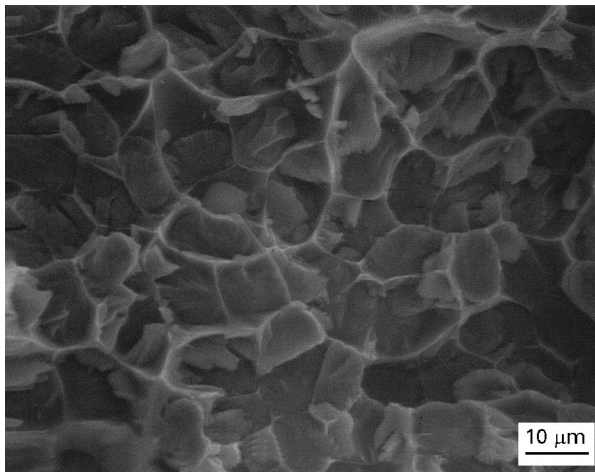


Figure 10 Fractograph of the 440/HPAL composite.

of broken fibres and the increased ductility of the matrix. The 440/HPAL composites also showed increased fibre fragmentation at the fracture surface. The increased ductility of the 440/HPAL will result in blunting of the crack tip slowing crack tip propagation. There was not a significant degree of fibre pullout in any of the composites tested. The lack of fibre pullout is due to the strong bonding of the fibres with the matrices used. Although not shown in the figures the composites also exhibited some cracking normal to the fracture surface. Some of these cracks went through the fibres. This also indicates good bonding is occurring. Some of this normal cracking was found in the 440/HPAL composite, but it was much more prevalent in the 440/6061 composite. The cracks were not as prevalent in the 440/HPAL composites due to the higher ductility of the matrix.

4. Conclusions

The 440/6061 composite was found to have inclusions segregated around fibres forming interconnected networks. The 440/HPAL composite had few inclusion in comparison to the 440/6061 composite.

The AE events of the 440/6061 composite had two distinct regions of events. The first region showed an exponential increase in the number of events. The events in this region were attributed to a dislocation activation mechanism. The second region of events were at a constant rate and continued to failure. The events in the second regions are attributed to be due to inclusion fracturing and some associated plastic deformation in the matrix.

The AE events in the 440/HPAL composite slowly increased until failure of the composite occurred. The events in this composite have been attributed with fibre breaking and some associated plastic deformation.

The 440/HPAL composite showed an increased number of AE events to failure. The increase in the number of events was attributed to the increased strain to failure of this material and an increase in the amount of damage.

Fibre failure propagates from one fibre to another leading to failure of the composite. The propagation is very rapid in the case of the 440/6061 composite due to the high strength and low ductility of the matrix. On the other hand the high ductility of the HPAL in the 440/HPAL composite slows the propagation down.

The fracture surfaces were relatively flat due to the rapid failure of the material. The fracture surfaces also showed plastic stretching of the matrix between the fibres and no fibre pullout. This indicates strong bonding is occurring between the fibres and the matrices.

Acknowledgements

The authors would like to acknowledge Professor J. Blucher for manufacturing the composites. The financial support of ARPA under grant MDA 972-93-1-0023 is gratefully acknowledged.

References

1. B. RAJ and B. B. JHA, *British J. NDT* **36** (1994) 16.
2. M. ARLINGTON, in "Nondestructive testing of fibre-reinforced plastics composites", Vol. 1, edited by J. Summerscales (Elsevier Applied Science, NY, 1987) pp. 25–63.
3. J. AWERBUCH and J. G. BAKUCKAS, "Metal matrix composites: testing, analysis and failure modes", edited by W. S. Johnson, ASTM STP 1032 (American Society for Testing and Materials, Philadelphia, PA, 1989) pp. 68–99.
4. M. MADHUKAR and J. AWERBUCH, in "Composite materials: testing and design" (seventh conference), edited by J. M. Whitney, ASTM STP 893, (American Society for Testing and Materials, Philadelphia, PA, 1986) pp. 337–367.
5. J. G. BAKUCKAS Jr., W. H. PROSSER and W. S. JOHNSON, *J. Compos. Mater.* **28** (1994) 305.
6. K. KOMAI, K. MINOSHIMA and T. FUNATO, in "Fractography of modern engineering materials, composites and metals", Vol. 2, edited by J. Masters and L. Gilbertson, ASTM STP 1203, (American Society for Testing and Materials, Philadelphia, PA, 1993) pp. 145–170.
7. D. A. ULMAN and E. G. HENNEKE II, in "Composite materials: testing and design" (sixth conference), edited by I. M. Daniel, ASTM STP 787, (American Society for Testing and Materials, Philadelphia, PA, 1982) pp. 323–342.
8. J. D. EASTERDAY, C. H. HENAGER, M. A. FRIESEL, R. H. JONES and M. T. SMITH, in "Proceedings of Nondestructive Evaluation and Material Properties of Advanced Materials", TMS annual meeting, New Orleans, edited by P. Liaw, O. Buck and S. M. Wolf, (1991) pp. 85–97.
9. P. M. MUMMERY, B. DERBY and C. B. SCRUBY, *Acta Metall. Mater.* **41** (1993) 1431.
10. C. R. HEIPLE, S. H. CARPENTER and M. J. CARR, *Metal Sci.* **15** (1981) 587.
11. C. B. SCRUBY, H. N. G. WADLEY, K. RUSBRIDGE and D. STOCKHAM-JONES, *ibid.* **15** (1981) 599.
12. H. C. KIM and T. KISHI, *Phys. Stat. Sol. (a)* **55** (1977) 189.
13. C. B. SCRUBY and H. N. G. WADLEY, *Philos. Mag. A* **44** (1981) 249.
14. D. FANG and A. BERKOVITS, *J. Mater. Sci.* **30** (1995) 3552.
15. S. McK. COUSLAND and C. M. SCALA, *Metal Sci.* **15** (1981) 609.
16. *Idem.*, *Mater. Sci. Engng.* **57** (1983) 23.
17. S. L. McBRIDE, J. W. MACLACHLAN and B. P. PARADIS, *J. Nondestructive Evaluation* **2** (1981) 35.
18. T. PACHECO, H. NAYEB-HASHEMI and H. E. M. SAL-LAM, *Int. J. Acoustic Emission* (in press).
19. C. McCULLOUGH, H. E. DEVE and T. E. CHANNEL, *Mater. Sci. Engng.* **189** (1994) 147.

20. A. S. ARGON, in "Composite materials Vol. 5, fracture and fatigue", edited by L. J. Broutman (Academic Press, NY, 1974).
21. S. OCHIAI and K. OSAMURA, *Metall. Trans. A* **21** (1990) 971.
22. M.-S. HU, J. YANG, H. C. CAO, A. G. EVANS and R. MEHRABIAN, *Acta Metall. Mater.* **40** (1992) 2315.
23. M. Y. HE, A. G. EVANS and W. A. CURTIN, *ibid.* **41** (1993) 871.
24. C. G. LEVI, G. J. ABBASCHIAN and R. MEHRABIAN, *Metall. Trans. A* **9A** (1978) 697.
25. W. F. SMITH, "Structure and properties of engineering alloys", 2nd Edn. (McGraw-Hill, NY, 1993).

*Received 23 July
and accepted 23 October 1996*